

Study of the angular coefficients and corresponding helicity cross sections of the W boson in hadron collisions

John Strologas*

Department of Physics and Astronomy, University of New Mexico, Albuquerque, New Mexico 87131, USA

Steven Errede

Department of Physics, University of Illinois at Urbana-Champaign, Urbana, Illinois 61801, USA

(Received 2 April 2005; revised manuscript received 22 December 2005; published 3 March 2006)

We present the standard model prediction for the eight angular coefficients of the W boson, which completely describes its differential cross section in hadron collisions. These coefficients are ratios of the W helicity cross sections and the total unpolarized cross section. We also suggest a technique to experimentally extract the coefficients, which we demonstrate in the Collins-Soper azimuthal-angle analysis.

DOI: [10.1103/PhysRevD.73.052001](https://doi.org/10.1103/PhysRevD.73.052001)

PACS numbers: 13.88.+e, 11.80.Cr, 12.15.-y, 12.38.-t

I. INTRODUCTION

The analytical study of the W boson is essential for the understanding of many open questions related to the electroweak physics, like the origin of the electroweak symmetry breaking and the source of the CP violation. Since its discovery the W hadronic cross section, mass, and width have been measured with great precision [1]. On the other hand complete physical information is contained in the boson's angular distribution in three dimensions, given by its differential cross section, which can be written as a sum of helicity cross sections. These quantities are related to the nature of the electroweak processes, the W polarization, and the presence of QCD effects. In this paper we address these issues in the case of W produced in hadron collisions.

The total differential cross section of the W production in a hadron collider, with a subsequent leptonic decay [2], is given by the equation:

$$\begin{aligned} \frac{d\sigma}{dq_T^2 dy d\cos\theta d\phi} = & \frac{3}{16\pi} \frac{d\sigma^u}{dq_T^2 dy} [(1 + \cos^2\theta) \\ & + \frac{1}{2}A_0(1 - 3\cos^2\theta) + A_1 \sin 2\theta \cos\phi \\ & + \frac{1}{2}A_2 \sin^2\theta \cos 2\phi + A_3 \sin\theta \cos\phi \\ & + A_4 \cos\theta + A_5 \sin^2\theta \sin 2\phi \\ & + A_6 \sin 2\theta \sin\phi + A_7 \sin\theta \sin\phi], \quad (1) \end{aligned}$$

where q_T and y are the transverse momentum and the rapidity of the W in the lab frame and θ and ϕ are the polar and azimuthal angles of the charged lepton from the W decay in the Collins-Soper (CS) frame [3]. The CS frame is used because in this frame we can experimentally reconstruct the azimuthal angle ϕ and the polar quantity $|\cos\theta|$. Our ignorance of the W longitudinal momentum, which is due to our inability to measure the longitudinal

momentum of its daughter neutrino in a hadron collider, introduces a two-fold ambiguity on the sign of $\cos\theta$. The quantity $d\sigma^u/dq_T^2 dy$ is the angles-integrated unpolarized cross section.

The dependence of the cross section on the leptonic variables θ and ϕ is completely manifest and the dependence on the hadronic variables q_T and y is completely hidden in the angular coefficients $A_i(q_T, y)$. This allows us to treat the problem in a model-independent manner since all the hadronic physics is described implicitly by the angular coefficients and it is decoupled from the well-understood leptonic physics. The angular coefficients are ratios of the W boson helicity cross sections and $d\sigma^u/dq_T^2 dy$. In order to explicitly separate the hadronic from the leptonic variables, the helicity amplitudes were used to describe the hadronic tensor associated with the hadronic production of the W [4]. The leptonic tensor on the other hand is analytically known, leading to analytic functions of the angles of the charged lepton in Eq. (1). It is common to integrate Eq. (1) over y and study the variation of the angular coefficients as a function of q_T .

If the W is produced with no transverse momentum, it is polarized along the beam axis because of the V-A nature of the weak interactions and helicity conservation. In that case A_4 is the only nonzero coefficient. If only valence quarks contributed to the W^\mp production, A_4 would equal 2, and the angular distribution (1) would be $\sim(1 \pm \cos\theta)^2$, a result that was first verified by the UA1 experiment [5].

If the W is produced with non-negligible transverse momentum, balanced by the associated production of jets, the rest of the angular coefficients are present and the cross section depends on the azimuthal angle ϕ as well. The last three angular coefficients— A_5 , A_6 , and A_7 —are nonzero only if gluon loops are present in the production of the W [6]. Hence, in order to study all the angular coefficients and associated helicity cross sections of the W in a hadron collider, we have to consider the production of the W with QCD effects at least up to order α_s^2 .

*Electronic address: strolog@fnal.gov

The importance of the determination of the W angular coefficients is discussed in [7], and is summarized here. This study allows us to measure for the first time the differential cross section of the W and study its polarization, since the angular coefficients are related to the helicity cross sections. It also helps us verify the QCD effects in the production of the W up to order α_s^2 . In addition, A_3 is only affected by the gluon-quark interaction and its measurement could constrain the gluon parton distribution functions. Moreover, the next-to-leading order (NLO) coefficients A_5 , A_6 , and A_7 are P -odd and T -odd and may play an important role in direct CP violation effects in W production and decay [6]. Finally, a quantitative understanding of the W angular distribution could be used to test new theoretical models and to facilitate new discoveries.

In this paper we present the standard model prediction for the angular coefficients A_i as a function of q_T , for proton-antiproton collisions at 1.8 TeV, using the DYRAD Monte Carlo program [8], an event generator of $W + \text{jet}$ up to order α_s^2 . Three of the coefficients, including A_4 which is the dominant one up to $q_T = 100$ GeV, are presented for the first time. We also suggest a new method for the extraction of the angular coefficients.

II. STANDARD MODEL PREDICTION FOR THE W ANGULAR COEFFICIENTS

In order to study the angular distribution of the W we have to choose a particular charge for the boson. In this paper we present the results for the W^- . The angular coefficients for the W^+ can be extracted by CP transformation. In the Collins-Soper frame, the CP transformation leaves ϕ unchanged and takes θ to $\pi - \theta$. If we assume that Eq. (1) describes W^- bosons, we have to change the sign of coefficients A_1 , A_4 , and A_6 , in order to describe W^+ bosons, without changing the definition of the Collins-Soper frame.

We generate Monte Carlo $W + \text{jet}$ events up to α_s^2 , including up to one gluon loop, from proton-antiproton collisions at $\sqrt{s} = 1.8$ TeV, using the DYRAD generator. We run with minimal kinematic and acceptance cuts, with a minimum transverse energy for the jet of 10 GeV and jet-jet angular separation of $\Delta R = \sqrt{(\Delta \eta_{\text{lab}})^2 + (\Delta \phi_{\text{lab}})^2} = 0.7$, in the pseudorapidity-phi space in the lab frame. A collection of parton distribution functions (PDF) were used [9].

We measure the θ and ϕ angles of the charged lepton in the Collins-Soper W rest-frame. At the Monte Carlo event-generator level, we know the momentum of the neutrino, so there is no two-fold ambiguity on the sign of $\cos\theta$. The CS frame is the rest-frame of the W where the z -axis bisects the angle between the proton momentum (\vec{p}_{CS}) and the opposite of the antiproton momentum ($-\vec{\bar{p}}_{\text{CS}}$) in the CS frame. The signs of the angular coefficients depend on the way the Collins-Soper x -axis and y -axis are defined. In this paper, we define them so that the x - z plane coincides with

the $p_{\text{CS}}\text{-}\bar{p}_{\text{CS}}$ plane and the positive y -axis has the same direction as $\vec{p}_{\text{CS}} \times \vec{\bar{p}}_{\text{CS}}$. The SM distribution of the ϕ and $\cos\theta$ for four q_T bins (15–25, 25–35, 35–65, and 65–105 GeV) is shown in Figs. 1 and 2, respectively. We note that at low transverse momentum of the W , the ϕ distribution is almost flat, whereas the $\cos\theta$ distribution almost follows the $(1 + \cos\theta)^2$ law. In the fourth q_T bin, there is a strong ϕ dependence of the cross section and the $\cos\theta$ distribution is almost a straight line ($|\cos\theta|$ is flat). There is a correlation between $\cos\theta$ and the W transverse mass M_T^W , with low $\cos\theta$ corresponding to low M_T^W events.

To calculate the angular coefficients from the angles of the charged lepton, we use the method of moments. We first define the *moment* of a function $m(\theta, \phi)$ as

$$\langle m(\theta, \phi) \rangle = \frac{\iint d\sigma(q_T, y, \theta, \phi) m(\theta, \phi) d\cos\theta d\phi}{\iint d\sigma(q_T, y, \theta, \phi) d\cos\theta d\phi}. \quad (2)$$

We can easily prove that

$$\begin{aligned} \langle m_0 \rangle &\equiv \langle \frac{1}{2}(1 - 3\cos^2\theta) \rangle = \frac{3}{20}(A_0 - \frac{2}{3}), \\ \langle m_1 \rangle &\equiv \langle \sin 2\theta \cos \phi \rangle = \frac{1}{5}A_1, & \langle m_2 \rangle &\equiv \langle \sin^2\theta \cos 2\phi \rangle = \frac{1}{10}A_2, \\ \langle m_3 \rangle &\equiv \langle \sin\theta \cos\phi \rangle = \frac{1}{4}A_3, & \langle m_4 \rangle &\equiv \langle \cos\theta \rangle = \frac{1}{4}A_4, \\ \langle m_5 \rangle &\equiv \langle \sin^2\theta \sin 2\phi \rangle = \frac{1}{5}A_5, & \langle m_6 \rangle &\equiv \langle \sin 2\theta \sin\phi \rangle = \frac{1}{5}A_6, \\ \langle m_7 \rangle &\equiv \langle \sin\theta \sin\phi \rangle = \frac{1}{4}A_7. \end{aligned} \quad (3)$$

For a set of discrete generator (or experimental) data, we substitute the integrals of Eq. (2) by sums and the cross

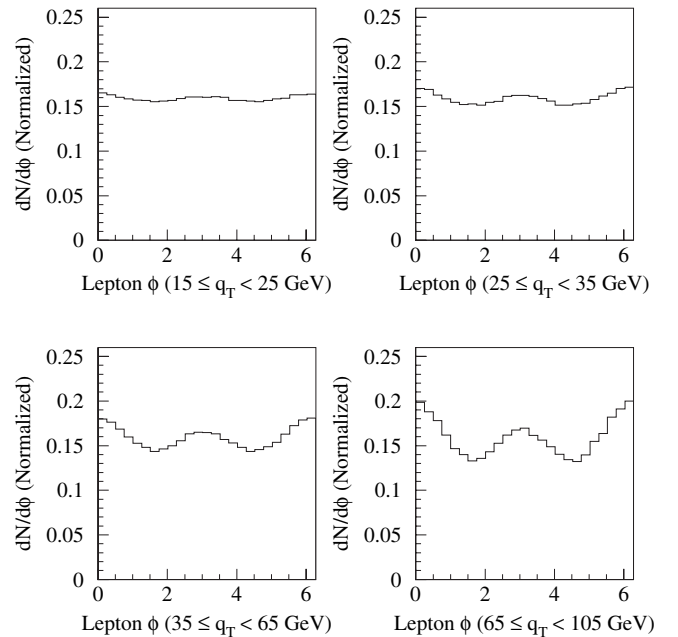


FIG. 1. The charged lepton ϕ distribution in the Collins-Soper W rest-frame for four q_T regions. The distributions are normalized to unity.

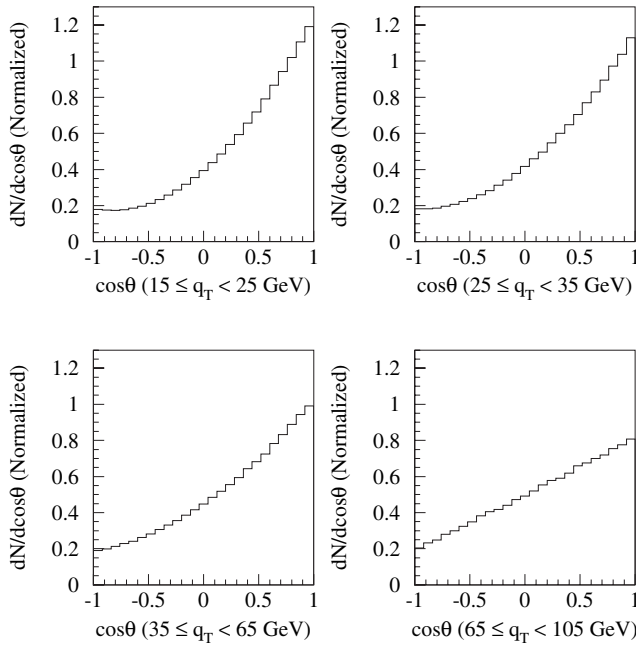


FIG. 2. The charged lepton $\cos\theta$ distribution in the Collins-Soper W rest-frame for four q_T regions. The distributions are normalized to unity.

section values by the weights w_i of the Monte Carlo events

$$\langle m(\theta, \phi) \rangle = \frac{\sum_{i=1}^N m(\theta_i, \phi_i) w_i}{\sum_{i=1}^N w_i}. \quad (4)$$

By solving Eqs. (3) for the angular coefficients and substituting the moments by the discrete expressions (4), we extract the standard model prediction. By ignoring the W rapidity, we actually calculate the y -integrated angular coefficients, which are now functions of just q_T . The results are shown in Figs. 3 and 4. The angular coefficients A_1 , A_4 , and A_6 are presented for the first time. The DYRAD Monte Carlo generator is more reliable for $q_T > 10$ GeV, which is also the transverse energy cut for our jets, and this value determines the minimum of our q_T -axis. The maximum is determined by the Monte Carlo statistics, which is also responsible for part of the uncertainty in the determination of the NLO and A_1 coefficients and respective helicity cross sections.

We notice that indeed A_4 is the only surviving major coefficient at low q_T values. It is also the only leading-order (LO) angular coefficient that decreases as q_T increases. The angular coefficient A_1 , although it is a LO coefficient, is much smaller than the other LO coefficients (A_0 , A_2 , A_3 , and A_4) and comparable to the NLO ones (A_5 , A_6 , and A_7). The coefficients A_0 and A_2 would be exactly equal if gluon loops were not included [2]. At order α_s^2 , A_0 is consistently greater than A_2 . There are relations that directly connect the angular coefficients with the helicity cross sections of the W boson [2]. We first extract the

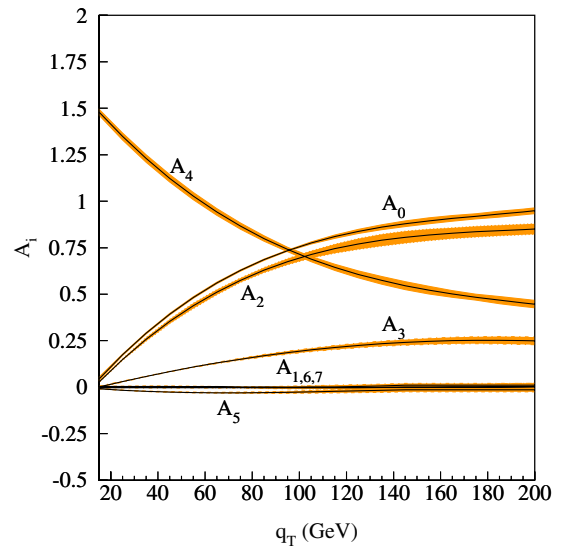


FIG. 3 (color online). The standard model prediction for the angular coefficients of the W produced in a collider at $\sqrt{s} = 1.8$ TeV. QCD effects are included up to order α_s^2 . The bands define the PDF and Q^2 systematics.

unpolarized cross section of the W as a function of q_T and using our prediction for the angular coefficients, we arrive at the standard model prediction for the W helicity cross sections at $\sqrt{s} = 1.8$ TeV, shown in Fig. 5. Here $d\sigma_i$ is the helicity cross section that corresponds to the angular coefficient A_i .

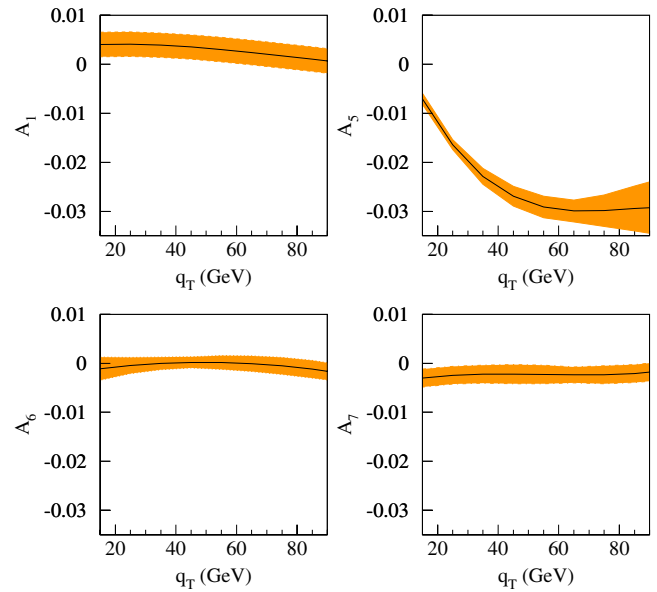


FIG. 4 (color online). The standard model prediction for the next-to-leading order coefficients (A_5 , A_6 , and A_7) and A_1 for the W production in a collider at $\sqrt{s} = 1.8$ TeV. QCD effects are included up to order α_s^2 . The T -odd and P -odd coefficients A_5 , A_6 , and A_7 are present only if gluon loops are included in the calculation. The bands define the PDF and Q^2 systematics.

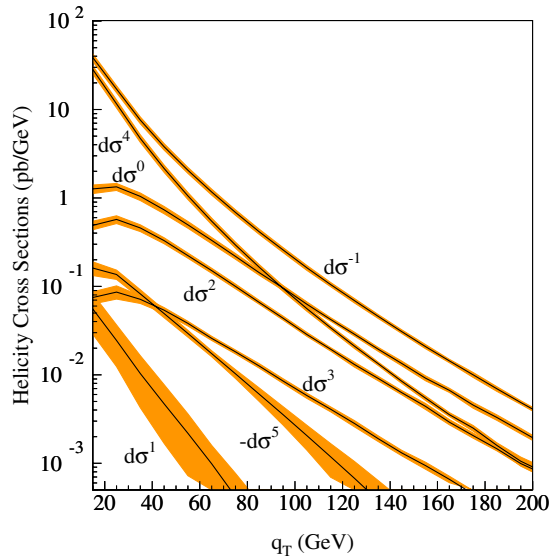


FIG. 5 (color online). The standard model prediction for the helicity cross sections of the W produced in a collider at $\sqrt{s} = 1.8$ TeV. QCD effects are included up to order α_s^2 . The bands define the PDF and Q^2 systematics.

III. EXPERIMENTAL DETERMINATION OF THE W ANGULAR DISTRIBUTION

E. Mirkes [2] first realized the problem of directly measuring the angular coefficients. The angular distributions of Figs. 1 and 2 are seriously distorted after the effects of the detector are considered and quality cuts are imposed on the data sample. To study the effect, we treat the generator leptons as electrons and we pass them through a detector simulator [12]. The new ϕ and $\cos\theta$ distributions are shown in Figs. 6 and 7, respectively. The shapes of the muon distributions are the same as that for electron $W + \text{jet}$ events, however less events are detected, because of the lower muon acceptance of a typical hadron collider detector. The main reason for the difference between Figs. 1, 2 and Figs. 6, 7 is the leptons transverse momentum cuts ($p_T^l > 20$ GeV and $p_T^{\nu} > 20$ GeV) and the charged lepton rapidity cut (central leptons are considered, $|y^l| < 1$).

The problem of distortion of the ϕ and $\cos\theta$ distributions due the detector effects and quality cuts is not the only one. A more fundamental problem is the actual measurement of these angles. To measure them, we need to reconstruct the W in the three-dimensional momentum space, in order to boost to its center of mass. The longitudinal momentum of the neutrino is not measured, but it is constrained by the mass of the W , based on equation:

$$p_z^{\nu} = \frac{1}{(2p_T^l)^2} (Ap_z^l \pm E^l \sqrt{A^2 - 4(p_T^l)^2 (p_T^{\nu})^2}), \quad (5)$$

where

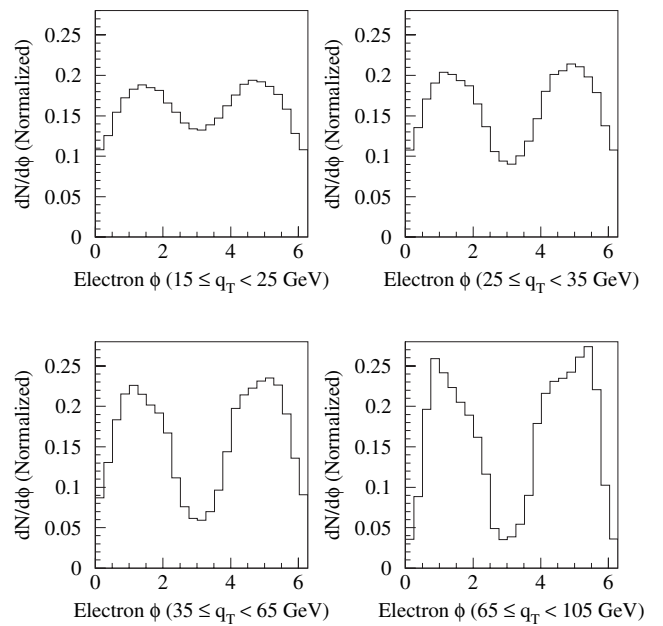


FIG. 6. The experimentally expected electron ϕ distribution in the Collins-Soper W rest-frame for four q_T regions. The muon distributions are almost identical. The distributions are normalized to unity.

$$A = M_W^2 + q_T^2 - (p_T^l)^2 - (p_T^{\nu})^2,$$

E^l is the energy of the charged lepton, p_T^l and p_T^{ν} are the transverse momenta of the charged lepton and the neutrino,

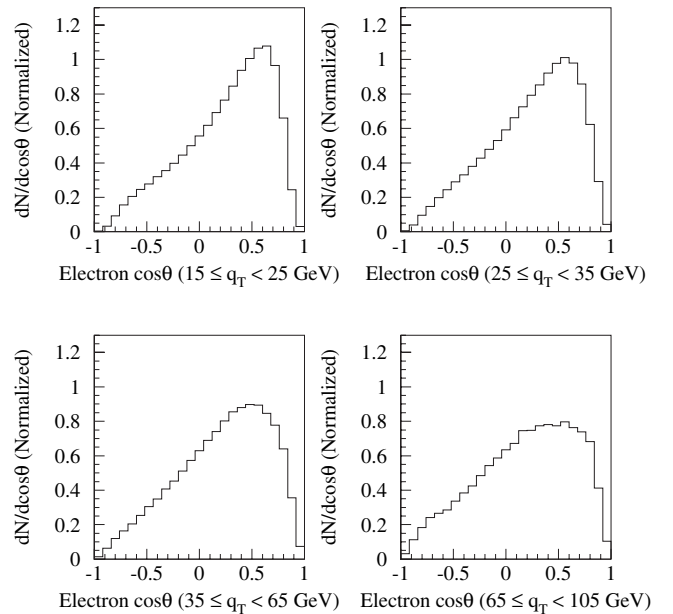


FIG. 7. The experimentally expected electron $\cos\theta$ distribution in the Collins-Soper W rest-frame for four q_T regions. The muon distributions are almost identical. The distributions are normalized to unity.

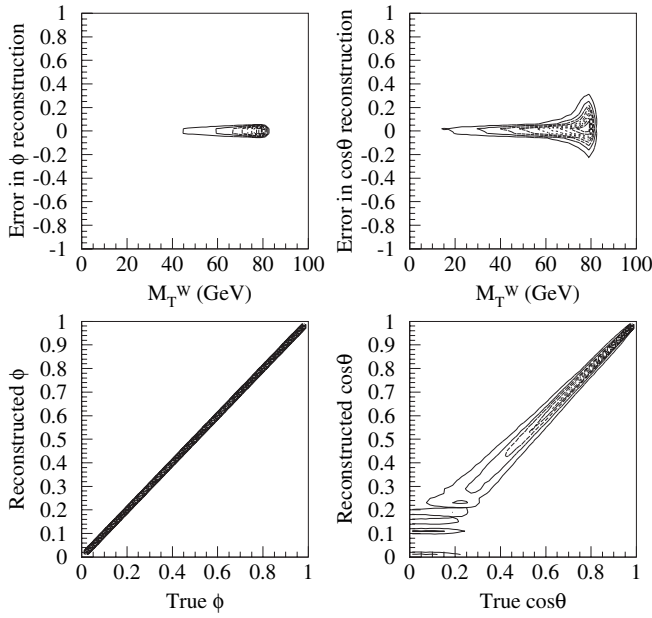


FIG. 8. The error in ϕ reconstruction due to the selection of the W mass is considerably lower than the error in $\cos\theta$ reconstruction, especially at high M_T^W values (upper plots). This corresponds to better reconstruction of the ϕ , while the $\cos\theta$ reconstruction is worse, especially at low values of $|\cos\theta|$ (lower plots).

and p_z^l is the longitudinal momentum of the charged lepton. The two solutions for the longitudinal momentum of the neutrino lead to two solutions for the W longitudinal momentum. Both solutions correspond to the same ϕ but to opposite $\cos\theta$ values.

Moreover, according to Eq. (5), for each event, we have to input a mass for the W to get p_z^l and eventually ϕ and $|\cos\theta|$. The mass of W is not known on event-by-event basis, we just know its pole mass and its Breit-Wigner width. Based on these two established values, we can plot the uncertainty in the measurement of ϕ and $|\cos\theta|$ introduced by the uncertainty in the mass of the W . For each Monte Carlo event we generate W masses that are greater than the transverse mass for the particular event and follow the Breit-Wigner distribution. In Fig. 8 we see that the systematic error on the measurement of ϕ is very small, but the $\cos\theta$ systematic error is significant, especially at low $|\cos\theta|$ and at big values of the transverse mass of the W . This makes the direct measurement of the $|\cos\theta|$ distribution more challenging.

IV. EXPERIMENTAL EXTRACTION OF THE ANGULAR COEFFICIENTS

In [7] it is suggested that the experimental distributions of Figs. 6 and 7 should be divided by the Monte Carlo distributions obtained using isotropic W decays. This method results in distributions similar to those shown in Figs. 1 and 2 and the extraction of the angular coefficients

is easier. Here we present a method that does not bias the experimental data by Monte Carlo data. Instead, it uses the knowledge of the detector and its effect on the theoretical distributions. We will demonstrate the method for the ϕ analysis.

If we integrate Eq. (1) over $\cos\theta$ and y , we get:

$$\frac{d\sigma}{dq_T^2 d\phi} = C'(1 + \beta_1 \cos\phi + \beta_2 \cos 2\phi + \beta_3 \sin\phi + \beta_4 \sin 2\phi), \quad (6)$$

where

$$C' = \frac{1}{2\pi} \frac{d\sigma}{dq_T^2}, \quad \beta_1 = \frac{3\pi}{16} A_3, \quad \beta_2 = \frac{A_2}{4}, \quad (7)$$

$$\beta_3 = \frac{3\pi}{16} A_7, \quad \beta_4 = \frac{A_5}{2}.$$

The observed ϕ distribution is given by Eq. (6), only if we ignore the effects of the detector and kinematic cuts. In any other case, there is an acceptance and efficiency function $ae(q_T, \cos\theta, \phi)$ which multiplies (1) before it is integrated over $\cos\theta$ and as a result, no angular coefficient is completely integrated out. In the actual data, what we measure is the number of events, which is:

$$N(q_T, \phi) = \int \frac{d\sigma}{dq_T d\phi d\cos\theta} ae(q_T, \cos\theta, \phi) d\cos\theta \int \mathcal{L} dt + N_{bg}(q_T, \phi), \quad (8)$$

where \mathcal{L} is the luminosity and $ae(q_T, \cos\theta, \phi)$ are the acceptances and efficiencies for the particular W transverse momentum and pixel in the $(\cos\theta, \phi)$ phase space. $N_{bg}(q_T, \phi)$ is the background for the given ϕ bin and q_T . If we combine Eqs. (8) and (1), then the measured distribution is:

$$N(q_T, \phi) = C' \left(f_{-1} + \sum_{i=0}^7 A_i f_i \right) + N_{bg}(q_T, \phi), \quad (9)$$

where $C' = C \int \mathcal{L} dt$, and f_i are the fitting functions, integrals of the product of the explicit functions of $\cos\theta$ and ϕ and the $ae(\cos\theta, \phi)$:

$$f_i(q_T, \phi) = \int_0^\pi g_i(\theta, \phi) ae(q_T, \cos\theta, \phi) d\cos\theta, \quad (10)$$

$$i = -1, \dots, 7,$$

where

$$g_{-1}(\theta, \phi) = 1 + \cos^2\theta, \quad g_0(\theta, \phi) = \frac{1}{2}(1 - 3\cos^2\theta),$$

$$g_1(\theta, \phi) = \sin 2\theta \cos\phi, \quad g_2(\theta, \phi) = \frac{1}{2} \sin^2\theta \cos 2\phi,$$

$$g_3(\theta, \phi) = \sin\theta \cos\phi, \quad g_4(\theta, \phi) = \cos\theta,$$

$$g_5(\theta, \phi) = \sin^2\theta \sin 2\phi, \quad g_6(\theta, \phi) = \sin 2\theta \sin\phi,$$

$$g_7(\theta, \phi) = \sin\theta \sin\phi.$$

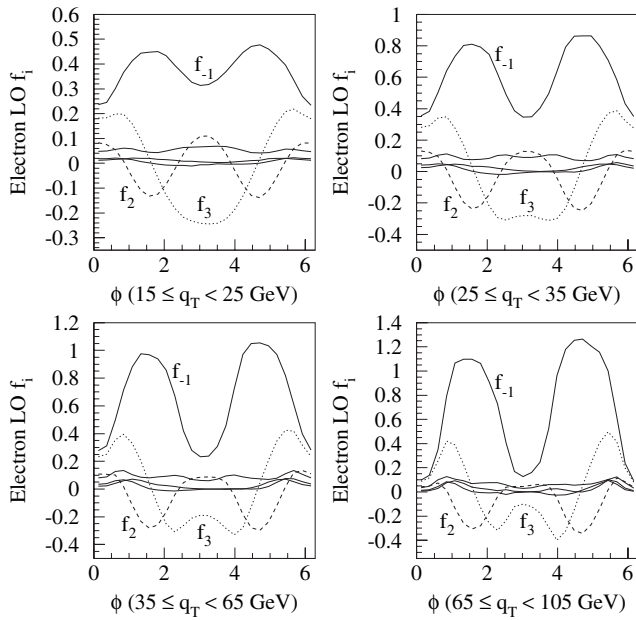


FIG. 9. The leading order $f_{-1,\dots,4}(\phi)$. These functions are multiplied by the respective W angular coefficients to give us the experimentally observable ϕ distributions.

The f_i functions can be calculated explicitly if we know the acceptance and the efficiency of the detector. Because we multiply by $ae(q_T, \cos\theta, \phi)$ before integrating over $\cos\theta$, no f_i is exactly zero. As a result, all coefficients are in principle measurable with the ϕ analysis and not just

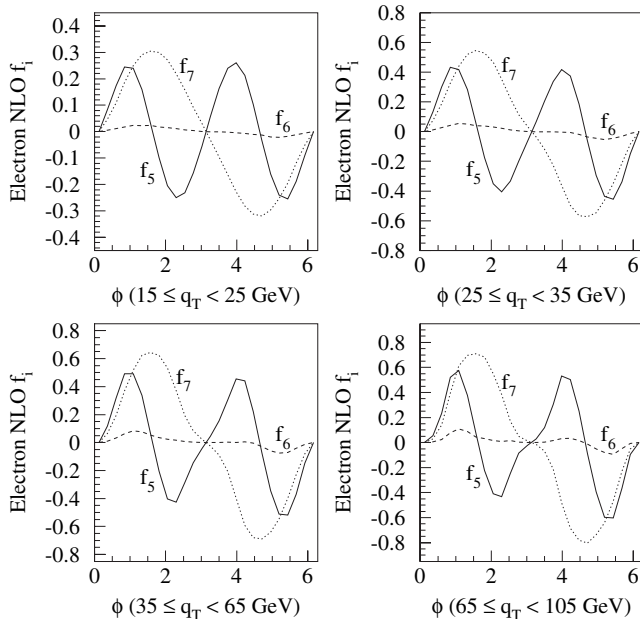


FIG. 10. The next-to-leading order $f_{5,6,7}(\phi)$. These functions are multiplied by the respective W angular coefficients to give us the next-to-leading order corrections to experimentally observable ϕ distributions.

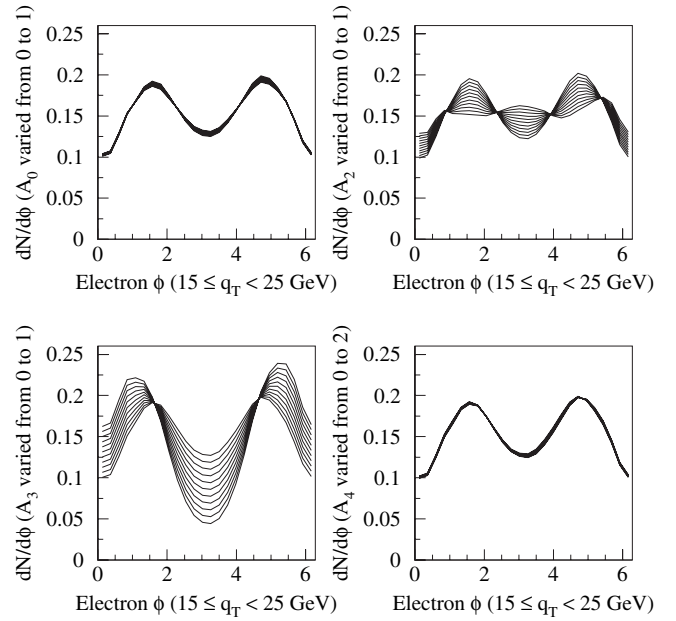


FIG. 11. The expected charged lepton ϕ distribution in the Collins-Soper W rest-frame for the first q_T bin, if we vary only one coefficient at the time (with a step of 0.1) and keep the rest at the standard model value. Only the A_2 and A_3 significantly affect the shape of the distributions. The same is true for the higher q_T bins.

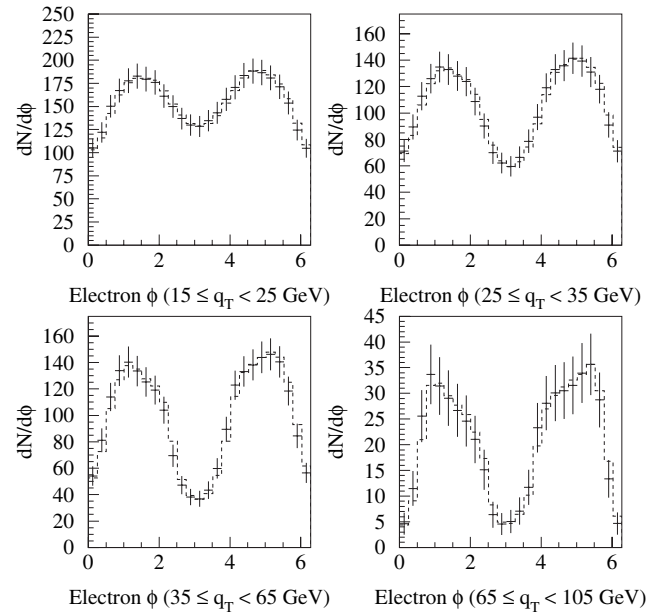


FIG. 12. The Monte Carlo prediction for the ϕ distribution, including the detector acceptance and efficiency, for the four q_T bins (points). The size of the sample and error bars correspond to the expected yields at the Tevatron at $\sqrt{s} = 1.8$ TeV). Also shown is the result of the fit (dashed line) using the theoretical prediction of Eq. (9) and varying A_2 and A_3 simultaneously. The backgrounds are ignored, only $W + \text{jet}$ events are considered.

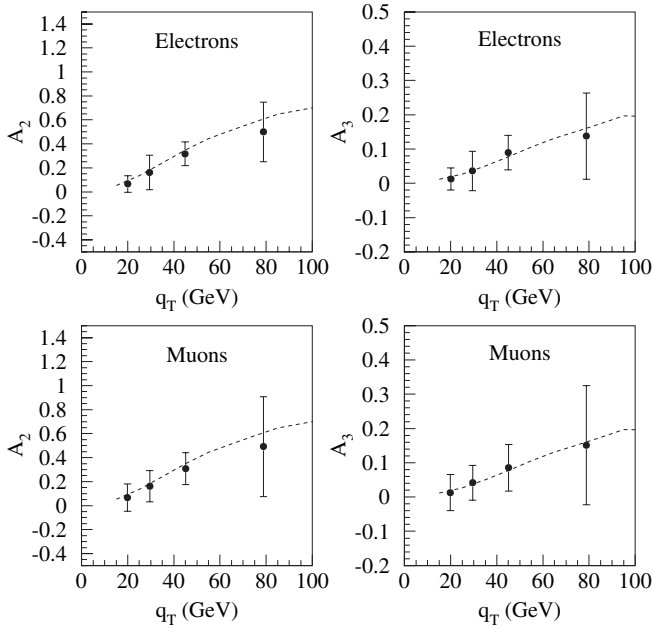


FIG. 13. The extracted angular coefficients, using the Monte Carlo data of Fig. 12 and fitting using the f_i functions. The angular coefficients that do not affect the shape of the ϕ distribution are kept at their standard model values. The error bars are statistical only.

A_2 and A_3 , as Eq. (6) suggests. In practice, the A_2 and A_3 are measurable with a greater statistical significance, because the terms $A_i f_i(\phi)$ are much smaller, for $i \neq 2, 3$. As a result, these terms affect less the ϕ distribution. Figures 9 and 10 show the f_i functions for electron acceptances and efficiencies. The shape of the f_i functions is almost identical for the muons. For perfect acceptance and no kinematic cuts ($ae = 1$), the only surviving f_i functions would be f_{-1} , f_2 , f_3 , f_5 , and f_7 , and they would be equal to $\frac{8}{3}$, $\frac{2}{3} \cos 2\phi$, $\frac{\pi}{2} \cos \phi$, $\frac{4}{3} \sin 2\phi$, and $\frac{\pi}{2} \sin 2\phi$, in accordance with Eq. (6). Figure 11 shows the ϕ distribution (9) for the lowest q_T bin, with the background neglected and with only one coefficient varying at a time. We see that the ϕ distribution is primarily sensitive to A_2 and A_3 , and these coefficients are the easier measurable ones with the ϕ analysis. Figure 12 shows the Monte Carlo expected experimental ϕ distributions for a data sample of the size of the Tevatron Run I.

The final step is to extract the angular coefficients using the pseudodata of Fig. 12. We keep the $A_{i \neq 2,3}$ coefficients frozen at their standard model values we determined above and we fit the distributions to the f_i varying A_2 and A_3 simultaneously. The result of the fit can be seen in Fig. 12 and the extracted coefficients in Fig. 13. We conclude that the measured angular coefficients are close to the values we extracted in Section II, verifying that the method is self-consistent and could be used for an experimental measurement of the W angular coefficients. The same technique can be applied in Z boson experimental studies—which do not demonstrate any problems in the kinematic reconstruction of the boson—using the future statistically significant datasets of the Tevatron and the LHC.

V. SUMMARY

The standard model prediction for the angular coefficients and the associated helicity cross sections of the W production in a hadron collider up to order α_s^2 in QCD and at $\sqrt{s} = 1.8$ TeV was presented. The experimental measurement of the angular distributions is distorted due to the acceptances and efficiencies of the detector and the application of quality cuts to reduce backgrounds. Two additional issues are the W mass width effect and the resolution of the two-fold ambiguity in the longitudinal momentum of the decay neutrino. We presented the effect of these factors on the angular distributions and noted that both problems do not affect the azimuthal angle of the charged lepton in the CS frame. Finally, we suggested a method of extracting the angular coefficients without having to divide the experimental data by Monte Carlo distributions of isotropic W decays. Passing the generator data through a detector simulator and analyzing the resulting data, we were able to get back the angular coefficients we determined from the direct analysis of the generator data, demonstrating that this procedure is reliable for the experimental measurement of the angular coefficients.

ACKNOWLEDGMENTS

We thank K. Hagiwara for initial discussions on this subject. We thank W. Giele for many helpful, stimulating discussions and DYRAD $W + \text{jet}$ Monte Carlo event generator support. We also thank U. Baur and T. Junk for their comments.

-
- [1] S. Eidelman *et al.* (Particle Data Group), Phys. Lett. B **592**, 1 (2004).
 - [2] E. Mirkes, Nucl. Phys. **B387**, 3 (1992).
 - [3] J.C. Collins and D.E. Soper, Phys. Rev. D **16**, 2219 (1977).
 - [4] C. S. Lam and W. K. Tung, Phys. Rev. D **18**, 2447 (1978).
 - [5] C. Albajar *et al.* (UA1 Collaboration), Z. Phys. C **44**, 15 (1989).
 - [6] K. Hagiwara, K. I. Hikasa, and N. Kai, Phys. Rev. Lett. **52**, 1076 (1984).
 - [7] E. Mirkes and J. Ohnemus, Phys. Rev. D **50**, 5692 (1994).
 - [8] W. T. Giele, E. W. N. Glover, and D. A. Kosower, Nucl.

- Phys. **B403**, 633 (1993).
- [9] We investigated a collection of parton distribution functions [10,11], CTEQ4M($\Lambda = 0.3$), CTEQM($\Lambda = 0.215$), CTEQM($\Lambda = 0.401$), *MRSA'*($\Lambda = 0.231$), all combined with Q^2 equal to the on-shell W boson mass squared. We also investigated CTEQ4M($\Lambda = 0.3$) with Q^2 equal to the dynamic W boson mass squared $(M_W^d)^2$, and Q^2 equal to $(M_W^d)^2 + q_T^2$.
- [10] H. L. Lai *et al.*, Phys. Rev. D **55**, 1280 (1997).
- [11] A. D. Martin, W. J. Stirling, and R. G. Roberts, Phys. Lett. B **354**, 155 (1995).
- [12] A Fast Monte Carlo simulator of the Run I CDF detector.